

## Selected topics from Belle

KAZUO ABE

High Energy Accelerator Research Organization, 1-1, Oho, Tsukuba, Ibaraki, 305-0801, Japan  
Email: kazuo.abe@kek.jp

**Abstract.** The Belle experiment continues to explore the origin of CP violation and test all aspects of standard model in  $B$  meson decays. Recent results on CP violating parameter  $\sin 2\phi_1$  and other measurements are presented.

**Keywords.**  $B$  meson; CP violation; Belle collaboration.

**PACS No.** 13.20.-v

### 1. Introduction

Presence of CP violation (breaking of symmetry when charge conjugation and parity operations are simultaneously applied) in the neutral  $B$  meson system was clearly established by recent  $\sin 2\phi_1$  measurements [1]. A good agreement of the measurement with a prediction based on global CKM fit suggests that the underlying cause of CP violation described by Kobayashi–Maskawa model is most likely the correct one. In this paper, I will first describe the  $\sin 2\phi_1$  measurement. Then I will describe other selected topics from recent Belle results that explore all aspects of standard model in  $B$  meson decays.

### 2. $\sin 2\phi_1$ measurement

It has been known that a clean observation of CP violation in the  $B$  meson system could first be observed in a difference of the time-dependent decay rates between  $B^0 \rightarrow J/\psi K_S$  and  $\bar{B}^0 \rightarrow J/\psi K_S$ .

$$\begin{aligned}\Gamma(B^0(\Delta t) \rightarrow J/\psi K_S) &\propto e^{-\Delta t/\tau_B} [1 - \sin 2\phi_1 \sin(\Delta m \Delta t)] \\ \Gamma(\bar{B}^0(\Delta t) \rightarrow J/\psi K_S) &\propto e^{-\Delta t/\tau_B} [1 + \sin 2\phi_1 \sin(\Delta m \Delta t)].\end{aligned}\quad (1)$$

Here  $\phi_1$  is one of the angles for the CKM unitarity triangle and  $\Delta m$  is  $B^0\bar{B}^0$  mixing parameter. Non-zero value of  $\sin 2\phi_1$  demonstrates a presence of CP violation.

We use  $J/\psi K_S$ ,  $\psi' K_S$ ,  $\chi_{c1} K_S$ ,  $\eta_c K_S$ ,  $J/\psi K^{*0}$ , and  $J/\psi K_L$ . These decay modes occur through a same quark-level transition  $b \rightarrow c\bar{c}s$ . Reconstruction of the decay modes except for  $J/\psi K_L$  is done by fitting the beam-energy constrained mass distribution to a signal peak

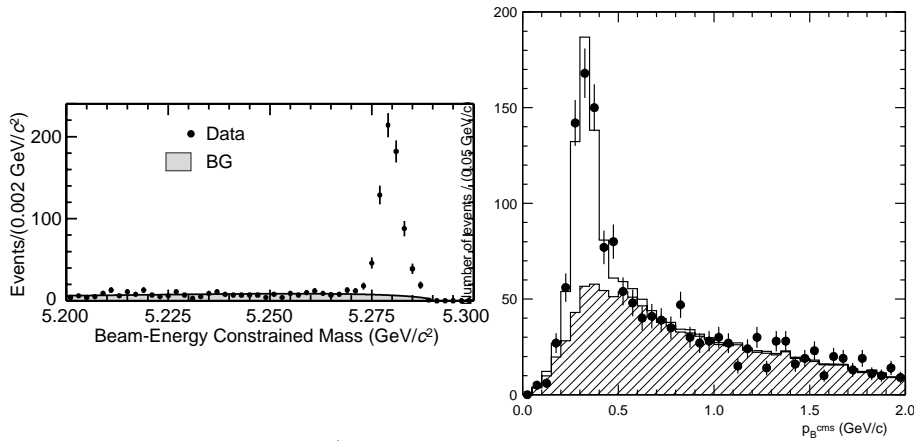


Figure 1.  $M_{bc}$  and  $p_B^*$  distributions.

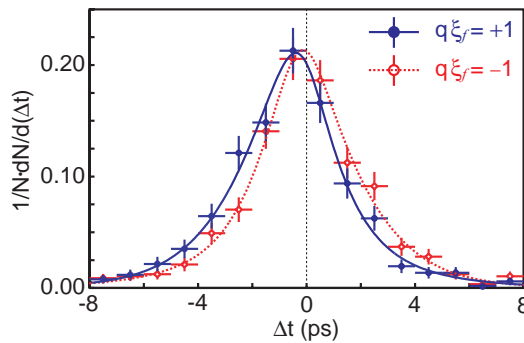


Figure 2.  $\Delta t$  distribution for  $q\xi_f = +1, -1$  data samples.

plus background (see figure 1). The case of  $J/\psi K_L$  must be treated separately because we cannot measure the  $K_L$  momentum. Here we assume a kinematics of two-body decay and compute the CM momentum of the reconstructed  $B$  (see figure 1). The signal peak is clearly visible at around 340 MeV/c.

For an event where one of  $B$  decaying to a CP final state is reconstructed, we compute its vertex and then determine the flavor and vertex of the other  $B$ . From these information, we can determine the initial flavor of  $B$  which decays to a CP final state after  $\Delta t$ . Performance of  $\Delta t$  measurement is tested by measuring the  $B^0\bar{B}^0$  mixing parameter and  $B$  lifetime. Method of flavor tagging is tested using the data sample of known flavor such as  $B^0 \rightarrow D^{*-} l^+ \nu$ . The wrong tagging fraction ( $w_l$ , where  $l$  is from 1 through 6 and indicates the quality of flavor tagging) is obtained from these analyses. The  $\Delta t$  distributions are shown in figure 2, where the data samples are combined into two categories using  $q\xi_f$ . Here  $q = +1(-1)$  if tagged as  $B^0(\bar{B}^0)$ , and  $\xi_f$  indicates the CP of final states.  $B^0 \rightarrow (c\bar{c})K_S$  and  $\bar{B}^0 \rightarrow J/\psi K_L$  decays take  $q\xi_f = +1$ , whereas  $\bar{B}^0 \rightarrow (c\bar{c})K_S$  and  $B^0 \rightarrow J/\psi K_L$  decays take  $q\xi_f = -1$ .

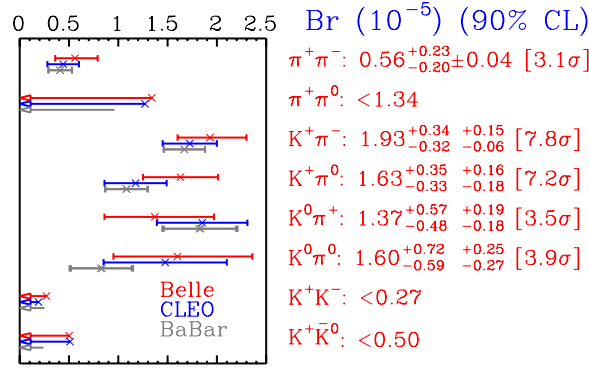


Figure 3. Belle results for  $\text{Br}(B \rightarrow K\pi, \pi\pi)$ .

We use unbinned maximum likelihood method for extracting  $\sin 2\phi_1$ . Probabilities of being signal and background are computed for each event using PDF (probability density function).

$$P_{\text{sig}}(\Delta t, q, w_l, \xi_f) = \frac{e^{-|\Delta t|/\tau_{B^0}}}{2\tau_{B^0}} [1 - \xi_f q (1 - 2w_l) \times \sin 2\phi_1 \sin(\Delta m \Delta t)]$$

$$P_{\text{bkg}}(\Delta t) = f_\tau \frac{e^{-|\Delta t|/\tau_{\text{bkg}}}}{2\tau_{\text{bkg}}} + (1 - f_\tau) \delta(\Delta t). \quad (2)$$

Using the detector resolutions,  $R_{\text{sig}}$  and  $R_{\text{bkg}}$ , the PDF for each event is given as

$$P_i = \int [f_{\text{sig}} P_{\text{sig}}(\Delta t') R_{\text{sig}}(\Delta t - \Delta t') + (1 - f_{\text{sig}}) P_{\text{bkg}}(\Delta t') R_{\text{bkg}}(\Delta t - \Delta t')] d\Delta t'. \quad (3)$$

We determine  $\sin 2\phi_1$  by maximizing  $L = \sum_i P_i$  ( $i$  each event) to be  $\sin 2\phi_1 = 0.99 \pm 0.14 \pm 0.06$ . CP violation in  $B$  meson system is clearly established.

### 3. $B \rightarrow \pi\pi, K\pi$

The  $B \rightarrow \pi\pi, K\pi$  decays generally contain both tree and penguin contributions. Since the tree diagram contains  $b \rightarrow u$  transition, effects of  $\phi_3$  (phase of  $V_{ub}$ ) can show up in the branching fractions through an interference between the two diagrams. Figure 3 summarizes the Belle results on the branching fraction measurements. They are in good agreement with BaBar and CLEO, and show a tendency of  $\text{Br}(KK) < \text{Br}(\pi^+\pi^-) < \text{Br}(K\pi)$ . We should note that  $\pi^+\pi^0$  is  $\simeq$  pure tree,  $K^0\pi^+$  and  $K^0\pi^0$  are  $\simeq$  pure penguin, and KKs contain annihilation and W-exchange.

Charge asymmetry due to direct CP violation in  $B \rightarrow K^\mp \pi^\pm$  is written as

**Table 1.** Belle results of  $A_{\text{CP}}(\%)$ .

Belle 90% CL (10.4 fb <sup>-1</sup> )	BBNS	KLS
-25 < $K^\mp \pi^\pm$ < 37	5 ± 9	-12.9 ~ -21.9
-40 < $K^\mp \pi^0$ < 36	7 ± 9	-10.0 ~ -17.3
-53 < $K^0 \pi^\mp$ < 82	1 ± 1	-0.6 ~ -1.5

$$A_{\text{CP}} = \frac{N(\bar{B} \rightarrow \bar{f}) - N(B \rightarrow f)}{N(\bar{B} \rightarrow \bar{f}) + N(B \rightarrow f)} = \frac{2 |T| |P| \sin \delta \sin \Delta\phi}{|T|^2 + |P|^2 + 2 |T| |P| \cos \delta \cos \Delta\phi} \simeq 2 \left| \frac{T}{P} \right| \sin \phi_3 \sin \delta \quad (4)$$

where  $\delta$  is a strong phase difference between the two diagrams, and  $\Delta\phi = \phi_T - \phi_P$ . Table 1 summarizes the Belle results for  $A_{\text{CP}}$  measurements. Here BBNS is for Beneke, Buchalla, Neubert and Sachrajda [2] and KLS is for Keum, Li and Sanda [3]. QCD factorization of BBNS predicts suppressed  $\delta$ , thus small  $A_{\text{CP}}$ , whereas pQCD of KLS predicts larger  $A_{\text{CP}}$ .

#### 4. $B \rightarrow D^{*\mp} \pi^\pm$

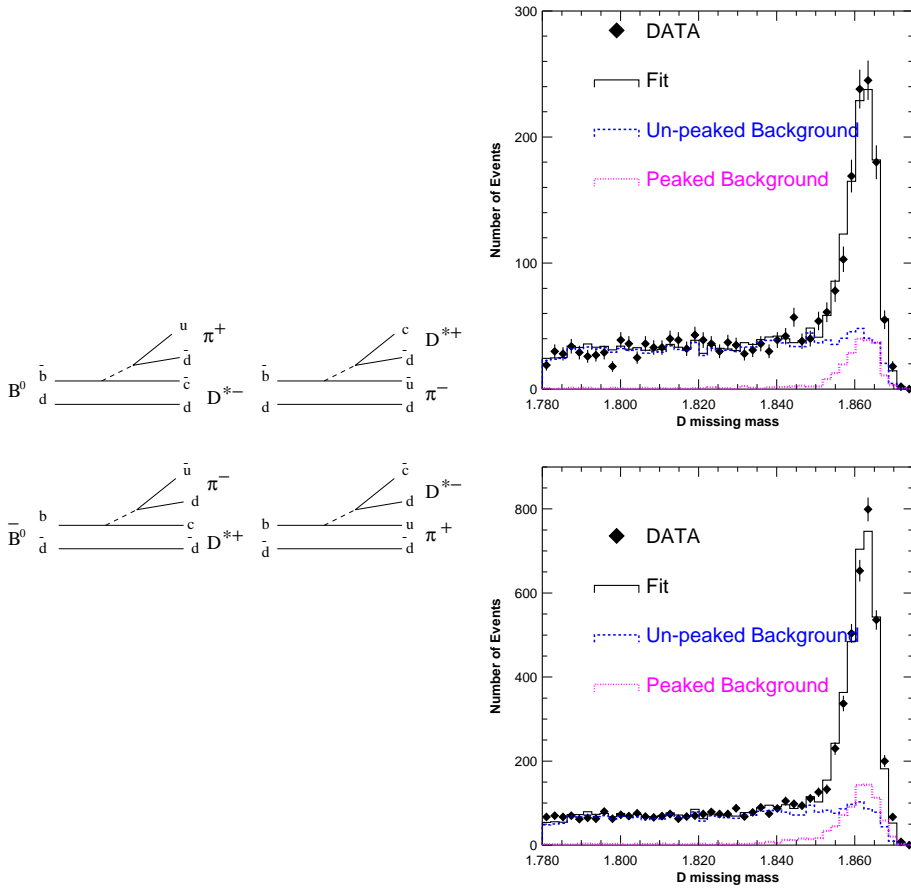
Decay amplitude for  $B^0 \rightarrow D^{*-} \pi^+$  is a sum of Cabbibo-favored decay (CFD) and doubly Cabbibo-suppressed decay (DCSD) through mixing, whereas that for  $B^0 \rightarrow D^{*+} \pi^-$  is a sum of DCSD and CFD through mixing. And likewise for the  $\bar{B}^0$  cases (see figure 4). Through a time-dependent analysis for these four decay rates, one can determine  $\sin(2\phi_1 + \phi_3)$  as well as  $\Delta m$ . We use a partial reconstruction technique for increasing the event statistics. We compute  $D$  missing mass using  $\pi_f$ ,  $\pi_s$ , and lepton from the process

$$B^0 \bar{B}^0 \rightarrow (l^+ X) + (D^{*+} (D^0 \pi_s^+) \pi_f^-), \quad B^0 B^0 \rightarrow (l^+ X) + (D^{*-} (\bar{D}^0 \pi_s^-) \pi_f^+). \quad (5)$$

Figure 4 shows the  $D$  missing mass distributions for the same-sign and opposite-sign data samples between  $\pi_f$  and lepton. From the  $\Delta z$  dependence of these data, we obtain  $\Delta m_d = 0.507 \pm 0.017(\text{stat}) \pm 0.019(\text{sys}) \text{ ps}^{-1}$ . Our next step is to extract  $\sin(2\phi_1 + \phi_3)$ . We estimate a sensitivity of  $\sin(2\phi_1 + \phi_3) \sim 0.35$  for 200 fb<sup>-1</sup> data.

#### 5. $B^0 \rightarrow \phi K_S$ and $B^0 \rightarrow D^{(*)+} D^{(*)-}$

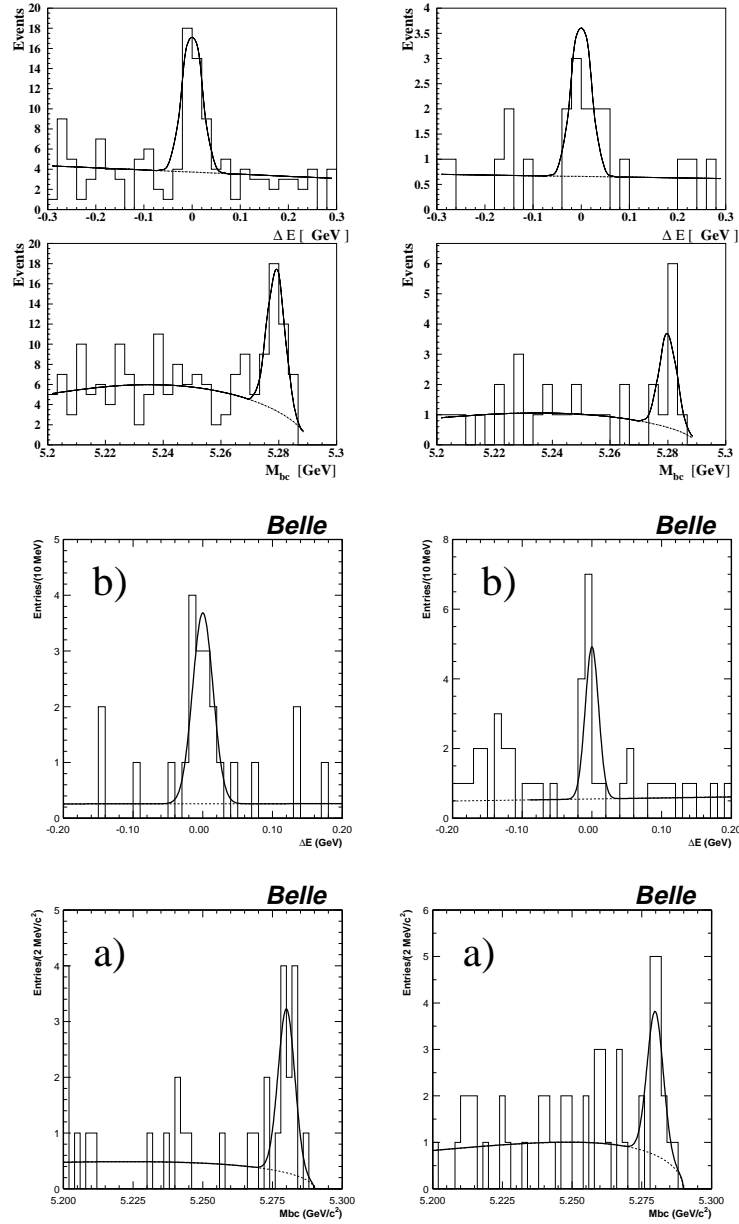
While the  $B \rightarrow J/\psi K_S$  leads to  $\sin 2\phi_1$  through the internal-tree diagram, the  $B^0 \rightarrow \phi K_S$  and  $B^0 \rightarrow D^{*+} D^{*-}$  lead to  $\sin 2\phi_1$  through the penguin and external-tree diagrams, respectively. It is interesting to see if they give the same  $\sin 2\phi_1$ . Although we observe clear signal peaks containing  $(8 \pm 3) \phi K_S$ ,  $(11.0 \pm 3.7) D^{*+} D^{*-}$ , and  $(11.2 \pm 4.0) D^{*+} D^-$  events based on the 21.6 fb<sup>-1</sup> data (figure 5), we still have some way before the  $\sin 2\phi_1$  measurements.



**Figure 4.** Diagrams for  $B \rightarrow D^* \pi$  decays (left), and  $D$  missing mass distributions for same-sign (top) and opposite-sign (bottom) events (right).

## 6. Radiative penguins, electroweak penguins

These decays occur through loop diagrams and therefore are good place to look for non-SM physics. Figure 6 (left) shows the  $M_{bc}$  distribution for  $B \rightarrow X_s \gamma$  candidates reconstructed by requiring one  $\gamma$ , one  $K$ , and up to four  $\pi$  (up to 1  $\pi^0$ ). We obtain  $106.5 \pm 16.8$  signal events from the  $5.8 \text{ fb}^{-1}$  data. Based on this, we determine  $\text{Br}(b \rightarrow s\gamma) = (3.36 \pm 0.53(\text{stat}) \pm 0.42(\text{sys})_{-0.54}^{+0.50}(\text{th})) \times 10^{-4}$ . The CLEO result and SM calculation are  $(3.19 \pm 0.43 \pm 0.27) \times 10^{-4}$  and  $(3.28 \pm 0.33) \times 10^{-4}$ , respectively. Agreement with SM is good, implying that a room for new physics in this mode is getting smaller. No signal is found for  $B \rightarrow \rho \gamma$  in the  $10.4 \text{ fb}^{-1}$  data. We set limits at  $\text{Br}(B^0 \rightarrow \rho^0 \gamma) < 10.6 \times 10^{-6}$  and  $\text{Br}(B^+ \rightarrow \rho^+ \gamma) < 9.9 \times 10^{-6}$ , which are still consistent with SM because the  $b \rightarrow d\gamma$  is suppressed with respect to  $b \rightarrow s\gamma$  by  $|V_{td}/V_{ts}|^2 \sim 20-50$ . Figure 6 (right) shows the  $M_{bc}$  plots for the  $B \rightarrow K^* \ell^+ \ell^-$  candidates in the  $29.1 \text{ fb}^{-1}$

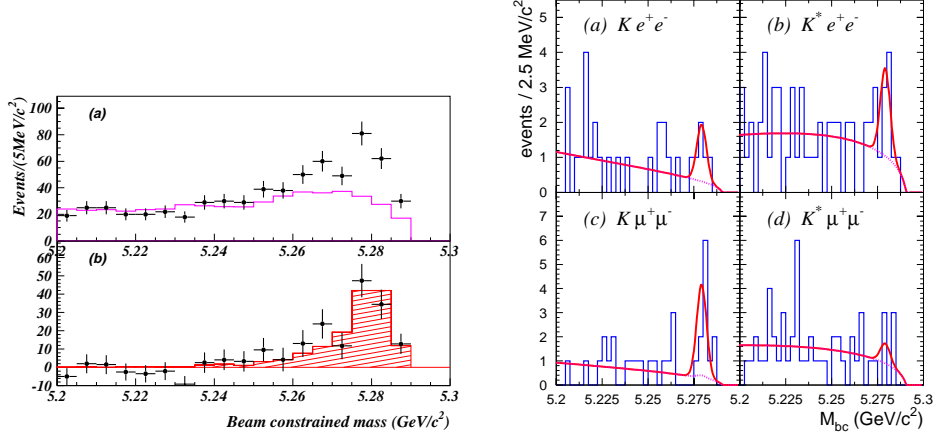


**Figure 5.**  $\Delta E$  and  $M_{bc}$  for  $\phi K^\pm$  (top-left),  $\phi K_S$  (top-right),  $D^{*+} D^{*-}$  (bottom-left), and  $D^{*+} D^-$  (bottom-right).

data. A clear signal peak is visible in the  $K\mu^+\mu^-$  mode with a  $4.7\sigma$  significance, from which we determine  $\text{Br}(B \rightarrow K\mu^+\mu^-) = (0.99^{+0.40}_{-0.32}(\text{stat})^{0.13}(\text{sys}) \times 10^{-6})$ . This is the first observation of the electroweak penguin decay.

**Table 2.**  $\text{Br}(B \rightarrow D^{(*)}K^-)$  in terms of ratios to  $D\pi$  modes.

$B(B^- \rightarrow D^0 K^-)/B(B^- \rightarrow D^0 \pi^-)$	$0.079 \pm 0.009 \pm 0.006$
$B(\bar{B}^0 \rightarrow D^+ K^-)/B(\bar{B}^0 \rightarrow D^+ \pi^-)$	$0.068 \pm 0.015 \pm 0.007$
$B(B^- \rightarrow D^{*0} K^-)/B(B^- \rightarrow D^{*0} \pi^-)$	$0.078 \pm 0.019 \pm 0.009$
$B(\bar{B}^0 \rightarrow D^{*+} K^-)/B(\bar{B}^0 \rightarrow D^{*+} \pi^-)$	$0.074 \pm 0.015 \pm 0.006$


**Figure 6.**  $M_{bc}$  before and after the background subtraction (left), and  $M_{bc}$  for  $K^{(*)}l^+l^-$  (right).

### 7. Cabbibo-suppressed $B \rightarrow D^{(*)}K^-$ decays

A naive factorization hypothesis predicts a suppression factor of  $B \rightarrow DK$  with respect to  $B \rightarrow D\pi$  to be  $(B \rightarrow D^{(*)}K^-)/(B \rightarrow D^{(*)}\pi^-) \simeq \tan^2 \theta_C (f_K/f_\pi)^2 \simeq 0.074$ . Belle results obtained from the  $10.4 \text{ fb}^{-1}$  data are summarized in table 2. They are in good agreement with the factorization expectation.

### 8. Color-suppressed $B \rightarrow D^0 \pi^0, D^{*0} \pi^0, D^0 \eta, D^0 \omega$ decays

These decays proceed through internal-tree diagrams (figure 7 (left)). Knowing their color-suppression factors are important for understanding the strong interaction effects in  $B$  decays. Belle results with the  $21.3 \text{ fb}^{-1}$  data give,  $\text{Br}(D^0 \pi^0) = (3.1 \pm 0.4 \pm 0.5) \times 10^{-4}$ ,  $\text{Br}(D^{*0} \pi^0) = (2.8^{+0.8+0.5}_{-0.7-0.6}) \times 10^{-4}$ ,  $\text{Br}(D^0 \eta) = (1.5^{+0.5}_{-0.4} \pm 0.3) \times 10^{-4}$ ,  $\text{Br}(D^0 \omega) = (1.8 \pm 0.5^{+0.4}_{-0.3}) \times 10^{-4}$ , respectively. They can be compared with factorization expectation [4] of 0.7, 1.0, 0.5, 0.7 (all with  $\times 10^{-4}$ ), respectively. Our results are consistently larger than factorization calculations.

### 9. Factorization in charmonium production

In factorization, the charmonium states in  $B$  decays appear through  $\langle [c\bar{c}] | \bar{c}(V_\mu - A_\mu)c | 0 \rangle$ . Here  $V_\mu$  can create  $J^{PC} = 0^{+-}, 1^{--}$  states only, and  $A_\mu$  can create  $J^{PC} = 0^{-+}, 1^{++}$

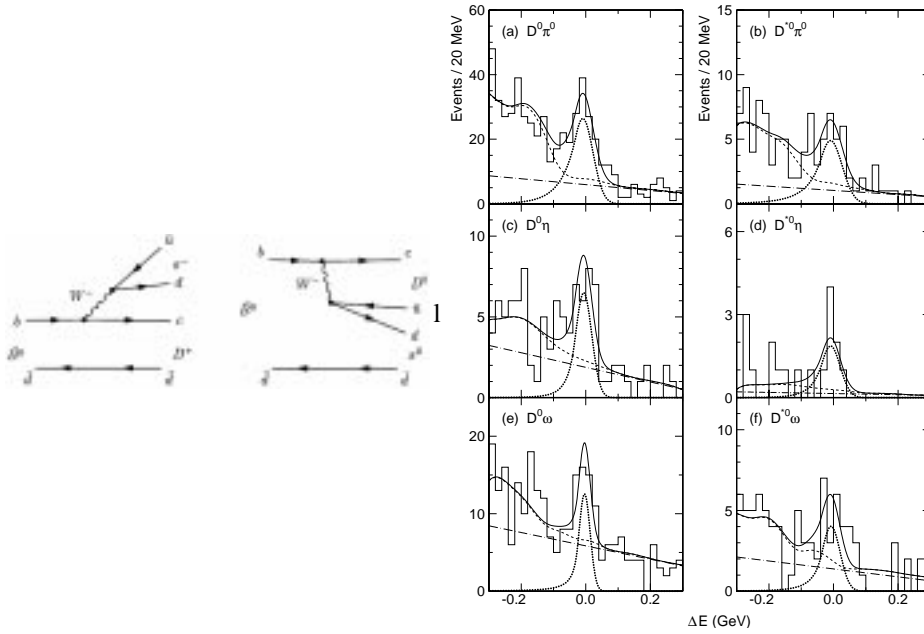


**Figure 7.** Diagrams for color-suppressed decays (*left*), and their  $\Delta E$  distributions (*right*).

only. Therefore, production of  $\chi_{c0}$  and  $\chi_{c2}$  states are not allowed. Our result of inclusive measurement using  $\chi_{c1,2} \rightarrow J/\psi\gamma(J/\psi \rightarrow l^+l^-)$  gives  $\text{Br}(B \rightarrow \chi_{c2}X) = (1.22 \pm 0.24 \pm 0.25) \times 10^{-2}$  and  $\text{Br}(B \rightarrow \chi_{c1}X) = (3.14 \pm 0.16 \pm 0.29) \times 10^{-2}$ . Exclusive measurement for  $B^+ \rightarrow \chi_{c0}K^+$  using  $\chi_{c0} \rightarrow \pi^+\pi^-$  gives  $(\text{Br}(B^+ \rightarrow \chi_{c0}K^+)/(\text{Br}(B^+ \rightarrow J/\psi K^+)) = 0.60^{+0.21}_{-0.18} \pm 0.05 \pm 0.08$ . It appears that the color-suppression factors for these decays are much smaller than what is expected from factorization.

## References

- [1] K Abe *et al* (Belle Collab.), *Phys. Rev. Lett.* **87**, 091802 (2001)  
B Aubert *et al* (BaBar Collab.), *Phys. Rev. Lett.* **87**, 091801 (2001)
- [2] M Beneke, G Buchalla, M Neubert and C T Sachrajda, *Nucl. Phys.* **B591**, 313 (2000)
- [3] Y Y Keum, H N Li and A I Sanda, *Phys. Rev.* **D63**, 054008 (2001)
- [4] M Neubert and B Stech, hep-ph/9705292